IPMU16-XXXX

LikeDM: likelihood calculator of dark matter detection

Xiaoyuan Huang[1*], Yue-Lin Sming Tsai[2†], and Qiang Yuan[3‡]

[1] *Physik-Department T30d, Technische Universität München, James-Franck-Straße, D-85748 Garching, Germany*

[2] *Kavli IPMU (WPI), University of Tokyo, Kashiwa, Chiba 277-8583, Japan*

[3] *Key Laboratory of Dark Matter and Space Astronomy, Purple Mountain Observatory, Chinese Academy of Sciences, Nanjing 210008, China*

(Dated: March 21, 2016)

With the large progresses of searching for dark matter (DM) particles from indirect and direct methods, we develop a numerical tool which enables fast calculation of the likelihood of specified DM particle models given a number of observational data, such as charged cosmic rays from space-borne experiments (e.g., PAMELA, AMS-02), γ-rays from Fermi space telescope, and the underground direct detection experiments. The purpose of this tool, LikeDM — likelihood calculator of dark matter detection, is to bridge the particle model of DM and the observational data. The intermediate steps between these two, including the astrophysical backgrounds, the propagation of charged particles, the analysis of Fermi γ-ray data, as well as the DM velocity distribution and the nuclear form factor, have been dealt with in the code. We release the first version (v1.0) focusing on the constraints of charged cosmic and gamma rays and the direct detection part will be implemented in the next version. This manual describes the framework, usage, and related physics of the code.

PACS numbers: 95.35.+d,96.50.S-

* huangxiaoyuan@gmail.com
† smingtsai@gmail.com
‡ yuanq@pmo.ac.cn

I. INTRODUCTION

With the discovery of the 125 GeV Higgs boson in the Large Hardon Collider [1, 2], we approaches a complete picture of the standard model (SM) of particle physics. The next step to go beyond the SM could be the identification of the dark matter (DM) particles which were suggested to be widely present in the Universe by a series of astronomical observations. Although the astronomical evidence can be attributed to the gravitational interaction between DM and SM particles, it is still not yet to exclude the possibility of weakly interacting massive particles (WIMPs). The potential weak interaction between DM and SM particles provides us with the opportunity to identify DM, via the direct collision between DM particles and the underground targets or the indirect products from DM annihilation or decay in the Universe. Many efforts have been paid to search for direct collisional signal of DM in underground detectors, however, no convincing evidence has been found [3–6]. On the other hand, with the operation of several new-generation space telescopes or detectors, such as PAMELA, AMS-02, and Fermi, many anomalies have been found in the high energy sky [7–9]. The uncertainties from the astrophysical background and/or astrophysical sources, however, make the identification of possible DM signal more ambiguous. Nevertheless, the constraints on DM models become more and more stringent with these new data, both direct and indirect. Some of the constraints depend on assumptions of the background contribution (e.g., the positron anomaly [10, 11]). Since there is no consistent signal from DM in all kinds of observations, we may expect that the assumption of astrophysical contribution to those anomalies is reasonable. The combination of various kinds of observations is expected to give much improved constraints on the DM models, which is one of the motivations that we develop this tool for DM likelihood calculation.

Another motivation is that it is non-trivial when confronting the DM model with the observational data due to the complicated astrophysical backgrounds. First, a proper modeling of the backgrounds, with possible systematic uncertainties (e.g., the cosmic ray (CR) propagation parameters), is necessary when calculating the likelihood of DM signal. Second, it is better to decouple the DM model inputs and the following astrophysical processes, which enables general application to any DM particle model. Third, we intend to have efficient computation of the DM signal as well as the backgrounds. With these purposes, we develop this likelihood calculator of DM detection, LikeDM. The basic function of LikeDM is to

deal with the intermediate steps between the input DM model and the data. To achieve this goal, we 1) calculate the propagation of CR electrons/positrons and antiprotons with Green's functions with respect to energy (e.g., integrated with space and time), 2) model the CR backgrounds with pheonomenological forms, 3) model the γ-ray emission with standard Fermi-LAT diffuse emission templates and point sources, and 4) calculate the likelihood map of γ-rays on the "energy$-$flux" plane for given regions of interest (ROIs). Some works have been published based on parts of these methods [12, 13]. Here we make this first version of this tool publically available in the community and summarize the details in this manual. The direct detection has not been included in this release, and will be added in the next version.

This manual is structured as follows. In Sec. II, we will describe the calculation of charged CRs from both the DM signal and the background. The Green's function for fast computation of the propagation of charged CRs will be presented. In Sec. III, we will describe the likelihood calculation from Fermi-LAT observations of dwarf spheroids (dSphs). We will give the energy$-$flux likelihood map with updated Fermi-LAT data. Finally, we will introduce the code, installation, and usage of LikeDM in Sec. IV, and summarize in Sec. V.

II. CHARGED COSMIC RAYS

A. Propagation of charged cosmic ray particles

The charged cosmic rays (CRs) propagate diffusively in the random magnetic field of the Milky Way. The interaction with the interstellar medium (ISM) will result in energy loss and/or fragmentation of the primary CRs, as well as the production of second CRs. For electrons/positrons, there will be additional energy loss due to the radiation in the interstellar radiation field (ISRF) and the magnetic field. The random shocks in the interstellar space may reaccelerate the low energy CR particles. There may also be convective transport of CRs as evidenced by the widely existence of galactic winds. The general propagation equation of CRs in the Milky Way can be written as [14]

$$\begin{aligned}\frac{\partial\psi}{\partial t} &= Q(\mathbf{x},p)+\nabla\cdot(D_{xx}\nabla\psi-\mathbf{V_c}\psi)+\frac{\partial}{\partial p}p^2D_{pp}\frac{\partial}{\partial p}\frac{1}{p^2}\psi\\ &- \frac{\partial}{\partial p}\left[\dot{p}\psi-\frac{p}{3}(\nabla\cdot\mathbf{V_c}\psi)\right]-\frac{\psi}{\tau_f}-\frac{\psi}{\tau_r},\end{aligned} \tag{1}$$

where ψ is the CR differential density per unit momentum interval, $Q(\mathbf{x}, p)$ is the source function, D_{xx} is the spatial diffusion coefficient, $\mathbf{V_c}$ is the convection velocity, D_{pp} is the diffusion coefficient in momentum space, $\dot{p} \equiv \mathrm{d}p/\mathrm{d}t$ is the momentum loss rate, τ_f and τ_r are time scales for fragmentation and radioactive decay respectively. A homogeneous spatial diffusion coefficient D_{xx} is assumed, and the rigidity dependence is assumed to be a power-law form $D_{xx} = D_0\beta(R/R_0)^\delta$, with β the velocity of the particle and δ reflecting the property of the ISM turbulence. For Kolmogrov type of the turbulence, we have $\delta = 1/3$. The reacceleration is described by the diffusion in momentum space. The momentum diffusion coefficient D_{pp} can be related with the spatial diffusion coefficient D_{xx} as [15]

$$D_{pp}D_{xx} = \frac{4p^2v_A^2}{3\delta(4-\delta^2)(4-\delta)w}, \tag{2}$$

where v_A is the Alfven speed, and w characterizes the level of turbulence which can be absorbed in v_A. The CRs are assumed to be confined in an extended halo with characteristic height z_h, beyond which free escape is assumed. Thus the major propagation parameters are D_0, δ, v_A, V_c and z_h.

The secondary-to-primary ratio, such as B/C and (Sc+Ti+V)/Fe, and the unstable-to-stable ratio of secondary particles, such as ^{10}Be/^{9}Be and ^{26}Al/^{27}Al are often used to determine the propagation parameters [15–18]. There are numerical codes to compute the CRs propagation in the Galaxy, such as GALPROP[1] [16] and DRAGON[2] [19].

In this tool, we adopt GALPROP version 50[3] to calculate the propagation of charged particles. We adopt 6 groups of propagation parameters with z_h varying from 2 kpc to 15 kpc which include the major uncertainties of the propagation parameters [20]. Such propagation parameters are consistent with the B/C data as well as the Fermi diffuse γ-ray emission [21].

B. Green's function of charged particle fluxes from DM

The annihilation or decay of DM particles in the Milky Way halo will produce charged CRs such as positrons and antiprotons, which will experience diffusive propagation before reaching the Earth. The fluxes of the charged CRs depend on both the density profile of

[1] http://galprop.stanford.edu/
[2] http://www.dragonproject.org/Home.html
[3] For the recent updated version 54 please refer to http://sourceforge.net/projects/galprop/

TABLE I: Propagation parameters

	D_0^a	z_h	v_A	δ
	(10^{28}cm^2 s^{-1})	(kpc)	(km s^{-1})	
1	2.7	2	35.0	0.33
2	5.3	4	33.5	0.33
3	7.1	6	31.1	0.33
4	8.3	8	29.5	0.33
5	9.4	10	28.6	0.33
6	10.0	15	26.3	0.33

[a]Diffusion coefficient at $R = 4$ GV.

DM and the propagation parameters (especially the height of the propagation halo z_h). We will consider several typically adopted forms of the DM density profiles, including the Navarro-Frenk-White (NFW) profile [22]

$$\rho_{\rm NFW}(r) = \frac{\rho_s}{(r/r_s)(1+r/r_s)^2}, \tag{3}$$

the Einasto (EIN) profile [23]

$$\rho_{\rm EIN}(r) = \rho_s \cdot \left[-\frac{2}{\alpha}\left(\left(\frac{r}{r_s}\right)-1\right)\right], \tag{4}$$

and the isothermal (ISO) profile [24]

$$\rho_{\rm ISO}(r) = \frac{\rho_s}{1+(r/r_s)^2}. \tag{5}$$

The profile parameters are given in Table II [25].

The source function of the charged CRs for DM annihilation or decay is

$$q(E,r) = \begin{cases} \frac{\langle\sigma v\rangle}{2m_\chi^2}\frac{dN}{dE} \times \rho^2(r), & \text{for anni.} \\ \frac{1}{m_\chi \tau}\frac{dN}{dE} \times \rho(r), & \text{for decay} \end{cases}, \tag{6}$$

where m_χ is the mass of the DM particle, $\langle\sigma v\rangle$ or τ is the annihilation cross section or decay lifetime, dN/dE is the particle yield spectrum per annihilation or decay.

The traditional way to solve the propagation of the DM induced charged particles is to incorporate the source term for given DM particle model in the propagation equation

TABLE II: DM density profile parameters

	r_s (kpc)	ρ_s (GeV cm^{-3})	α
NFW	20	0.26	...
EIN	20	0.06	0.17
ISO	5	1.16	...

Eq. (1). In order to isolate the DM particle model from the propagation calculation, we approximate the function dN/dE with a series of Gaussian kernel functions

$$\frac{dN}{dE} \approx \sum_i C_i K_i(E, E_i) = \sum_i \frac{C_i}{\sqrt{2\pi}\sigma_i} \exp\left[-\frac{(E-E_i)^2}{2\sigma_i^2}\right], \tag{7}$$

where E_i and σ_i are the central value and width of the ith Gaussian kernel. We find that generally $\sigma_i = 15\%E_i$ can give good approximation to most of the energy spectrum dN/dE, except that it has very distinct spectral structures (e.g., monochromatic). The left panel of Fig. 1 shows an illustration of the kernel functions weighted by the coefficients C_i for a given spectrum. We can then calculate the propagated spectrum of each kernel function, $G_i(E)$, which is the approximate Green's function with respect to energy E (dashed lines in the right panel of Fig. 1). The total propagated spectrum can be obtained as

$$\Phi(E) \approx \sum_i C_i G_i(E). \tag{8}$$

As shown in the right panel of Fig. 1, the result from this Green's function method is well consistent with the direct calculation of the propagation (red dots).

Applying this trick, any DM spectrum at the Earth can be easily and fast obtained by inserting its DM source shape. This helps us to much reduce the numerical computation time if the predetermined Green's function table is given. Users are allowed to generate their own tables of Green's function by using various propagation codes and then fed them into LikeDM.

C. Backgrounds

The CR backgrounds relevant for the DM searches include the primary electrons from the CR sources, the secondary positrons and antiprotons from interactions between the pri-

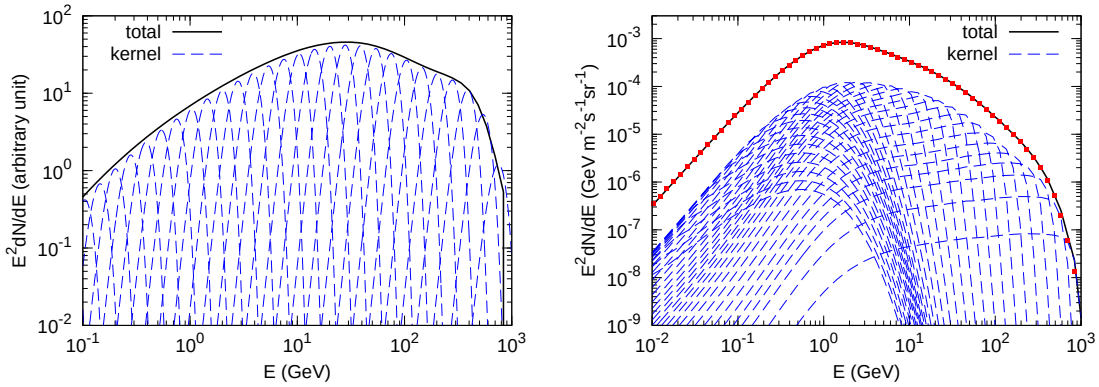

FIG. 1: Illustration of the kernel functions and the sum of the positron spectra, before (left) and after (right) the propagation. The points in the right panel show the direct caculation of the propagated spectrum of positrons with GALPROP. Here we adopt the second setting of the propagation parameters, and NFW profile of DM density. The mass of DM particle is adopted to be 1 TeV, with annihilation cross section $\langle\sigma v\rangle = 10^{-26}$ cm^{3}s^{-1} and annihilation final state $b\bar{b}$. *** **Sming: A bit worried about the *arbitrary unit*. May Qiang make it clear? ***

mary CR nuclei and the ISM, as well as the possible primary sources of positrons from e.g., pulsars [26]. Instead of using the more physical model considering the injection/production and propagation of each type of particles [27, 28], we adopt an empirical model to fit the locally observed cosmic ray fluxes following Ref. [11]. This is equivalent to assume that no DM "signal" in the current data has been found and all the measured events come from CR backgrounds (see also [29]). Slightly different from that of Ref. [11], we assume broken power-law forms to describe the fluxes of the primary electrons, secondary positrons/electrons and secondary antiprotons, with the purpose to reproduce the wide band data:

$$\phi_{e^-} = C_{e^-} E^{-\gamma_1^{e^-}} \left[1 + (E/E_{\rm br}^{e^-})^{\gamma_2^{e^-}}\right]^{-1}, \quad (9)$$

$$\phi_{e^+} = C_{e^+} E^{-\gamma_1^{e^+}} \left[1 + (E/E_{\rm br}^{e^+})^{\gamma_2^{e^+}}\right]^{-1}, \quad (10)$$

$$\phi_{\bar{p}} = C_{\bar{p}} E^{\gamma_1^{\bar{p}}} \left(1 + E/E_{\rm br}^{\bar{p}}\right)^{-\gamma_2^{\bar{p}}}. \quad (11)$$

Note the form of antiprotons is slightly different from that of electrons and positrons in order to better fit the data. The secondary electron spectrum is assumed to be the same as the secondary positron spectrum, with a normalization factor 0.6 as expected from the pp collision [30]. As for the extra source to reproduce the electron/positron excess, the same

power-law with exponential cutoff is assumed

$$\phi_s = C_s E^{-\gamma_s} \exp(-E/E_c). \tag{12}$$

Therefore the total fluxes of positrons, electrons, positrons + electrons are

$$\Phi_{e^+} = \phi_{e^+} + \phi_s, \tag{13}$$

$$\Phi_{e^-} = \phi_{e^-} + 0.6\phi_{e^+} + \phi_s, \tag{14}$$

$$\Phi_{e^\pm} = \phi_{e^-} + 1.6\phi_{e^+} + 2\phi_s, \tag{15}$$

and the positron fraction is $\Phi_{e^+}/\Phi_{e^\pm}$, respectively.

The data used to fit the backgrounds include the updated AMS-02 positron fraction [31], the AMS02 spectra of electrons and positrons [32], the AMS-02 total $e^\pm$ spectra [33], and the PAMELA antiproton spectrum [34]. The AMS-02 data below 1 GeV are excluded in the fitting [11]. The empirical background model gives very good description to the data, as shown in Fig. 2. The best-fitting χ^2 value over the number of degree-of-freedom (dof) is about 132.8/285 for e^+e^- and about 11.1/19 for antiprotons. The best-fitting parameters are given in Table III.

TABLE III: Best-fitting parameters of the backgrounds

	C	γ_1	γ_2	$E_{\rm br}$	E_c
	($\rm GeV^{-1}m^{-2}s^{-1}sr^{-1}$)			(GeV)	(GeV)
ϕ_{e^-}	21.6701	0.9344	2.3734	3.6390	...
ϕ_{e^+}	1.4991	0.9024	2.3647	2.8434	...
ϕ_s	0.6526	2.3390	...	...	652.89
$\phi_{\bar{p}}$	0.0995	1.844	5.077	2.849	...

When the DM component is added in the model, we should allow some freedom of the backgrounds to get a global best-fitting to the data. Therefore we multiply factors $\alpha_i E^{\beta_i}$, with $i = \{e^-, e^+, s, \bar{p}\}$, on the primary electrons, the secondary positrons/electrons, the extra positrons/electrons and the secondary antiprotons. We adopt the profile likelihood method to manage the nuisance parameters α_i and β_i, with the scan ranges [0.1, 10] and [−0.5, 0.5], respectively. The code `Minuit` [35] is used for finding the maximum likelihood but users can easily replace it by other similar codes.

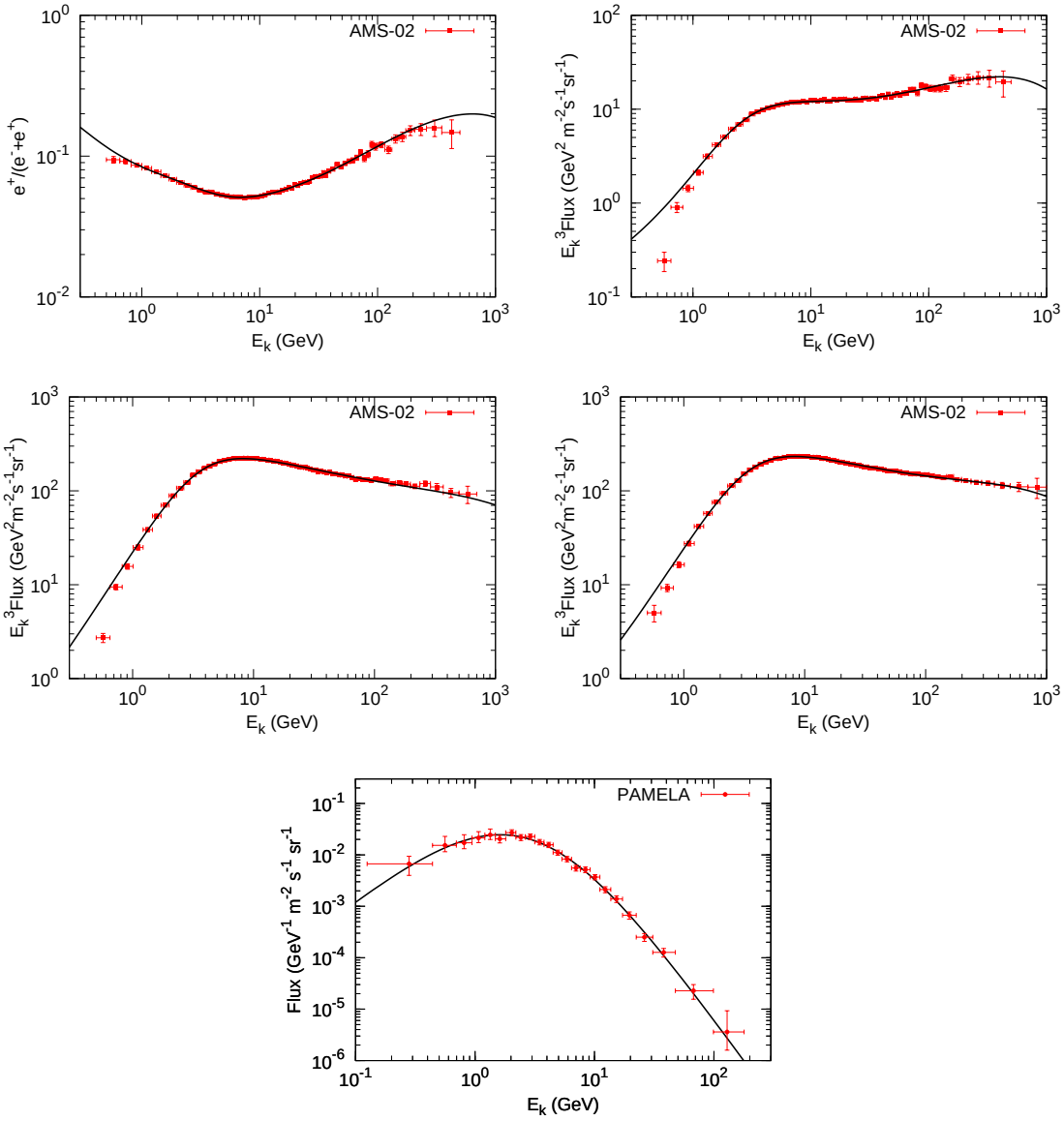

FIG. 2: Background fitting results of the positron fraction (top-left), positron (top-right), electron (middle-left), total $e^{\pm}$ (middle-right), and antiproton spectra (bottom).

D. Solar modulation

The low energy charged CRs will be modulated by the solar activities. We adopt the simple force-field approximation with only one parameter, the modulation potential, to calculate the effect of the solar modulation [36]. Since our background model is an empirical one instead of a physical model, the solar modulation only applies on the CR fluxes from the DM annihilation or decay.

E. Examples on DM constraints

In this subsection we present some results on the DM model parameter constraints from charged CRs derived with the above method. We adopt DM annihilation scenario for illustration, and assume the DM density profile is NFW. Given one set of the DM model parameters, such as the mass, the annihilation cross section, and the branching ratios to each annihilation channel, we calculate the production spectra of positrons and antiprotons using the tables of Ref. [37]. The propagated fluxes, calculated with the above described Green's function method, together with the backgrounds, are then incorporated in the data to derive the likelihood, $\mathcal{L} \propto \exp(-\chi^2/2)$, of this particular set of DM parameters.

The top-left panel of Fig. 3 shows a map of $-2\Delta\ln(\mathcal{L}) \equiv -2\ln(\mathcal{L}/\mathcal{L}_{\rm best})$, where $\mathcal{L}$ is the likelihood of the model with different value of $\langle\sigma v\rangle$ for given m_χ, and $\mathcal{L}_{\rm best}$ is the maximum likelihood for this particular mass. The likelihood is calculated using the AMS-02 e^+e^- data. The propagation model is #2, the solar modulation potential is 0.5 GV, and the DM annihilation channel is assumed to be $\tau^+\tau^-$. The dashed line shows the 95% confidence level (CL) upper limits, defined with $-2\Delta\ln(\mathcal{L}) = 2.71$ for a single-sided probability distribution. Other panels of Fig. 3 illustrate the 95% upper limits of the DM annihilation cross section for different channels (top-right), propagation models (bottom-left), and solar modulation potentials (bottom-right).

III. GAMMA-RAYS FROM DSPHS

Gamma-rays are another very important messenger for the indirect detection of DM. Gamma-rays travel through the space without deflection, thus they can point back to the sources emiting them. It is possible to choose optimal regions in the sky with high DM density and low astrophysical background to search for DM. The dSphs in the Milky Way are widely believed to be favorable targets with high signal-to-noise ratio. Many works have been performed to search for DM-induced γ-rays from dSphs with Fermi-LAT data, yet none of them reported a significant detection [38–42]. Recently the ongoing Dark Energy Survey (DES) reported some new candidates of dSphs in the southern-hemisphere [43, 44]. Several groups had claimed possible weak γ-ray signals from Reticulum 2 [45] and Tucana III [46]. Since there are no reliable kinematics (hence DM density profiles) measurements available

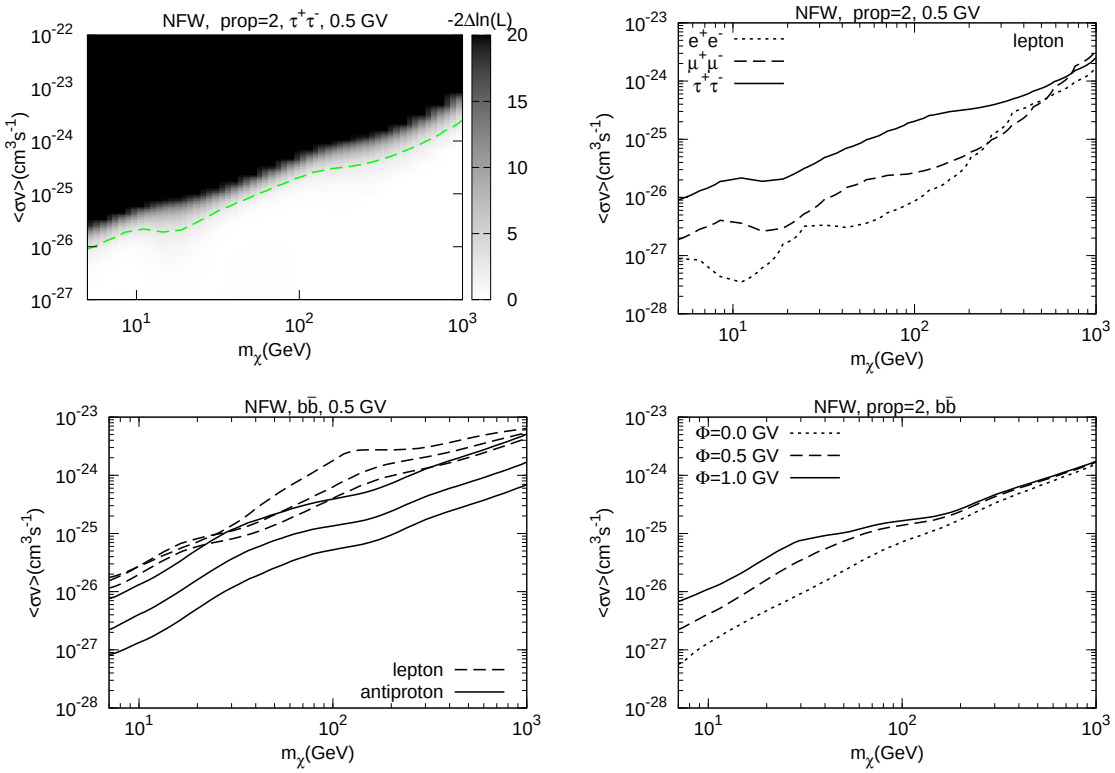

FIG. 3: Constraints on the DM annihilation parameters from the charged CR data. The DM density profile is assumed to be NFW, and the solar modulation potential is adopted to be 0.5 GV unless stated elsewhere. Top-left: the map of $-2\Delta\ln(\mathcal{L})$ on the (m_χ, $\langle\sigma v\rangle$) plane from the AMS-02 lepton data, for DM annihilation into $\tau^+\tau^-$. The dashed line shows the 95% CL limits. Top-right: 95% upper limits of $\langle\sigma v\rangle$ from the AMS-02 lepton data, for different DM masses and the annihilation channels of e^+e^-, $\mu^+\mu_-$, and $\tau^+\tau^-$, respectively. Bottom-left: 95% upper limits of $\langle\sigma v\rangle$ from the AMS-02 lepton data (dashed) and the PAMELA antiproton data (solid), for DM annihilation to $b\bar{b}$. The three lines of each group from top to bottom represent the propagation models #1, #2, and #6, respectively. Bottom-right: 95% upper limits of $\langle\sigma v\rangle$ from the combination of the AMS-02 lepton data and the PAMELA antiproton data, for DM annihilation into $b\bar{b}$. The three lines from top to bottom represent the solar modulation potentials of 1.0, 0.5, and 0 GV, respectively.

for these newly-discovered dSphs candidates, the constraints or implication on DM from them are very uncertain. Here we adopt the dSphs sample of Ref. [41] in LikeDM.

A. Likelihood Map

To ensure an easy computation of the total likelihood for any given shape of the γ-ray spectrum, we take the likelihood map method first proposed in our work Ref. [12] and further developed in Refs. [39, 41]. Briefly speaking, the likelihood $\mathcal{L}_{ij}$ of any flux ϕ_j in each energy bin $[E_{i-1/2}, E_{i+1/2}]$ is calculated to give a likelihood map on the (E, ϕ) plane. The total likelihood of a given spectrum can be simply obtained through a product of the likelihoods over all energy bins. This method is DM particle model independent, flexible and time-saving. Also as shown in Ref. [47], it is simple to be extended to incorporate with data from other observations.

We describe the method in more detail. DM annihilation in dSphs is adopted for illustration.[4] The case of DM decay can be easily obtained via proper re-adjustment of the formula (see e.g., Eq. (6)). The γ-ray flux from the annihilation of DM in a dSph is

$$\phi(E) = \frac{\langle \sigma v \rangle}{8\pi m_\chi^2} \times \frac{dN_\gamma}{dE_\gamma} \times J, \tag{16}$$

where $J = \int dl d\Omega \rho(l)^2$ is the so-called J-factor which characterizes the amount of annihilation from specified direction given the density distribution ρ of DM. For each energy bin $[E_{i-1/2}, E_{i+1/2}]$, we approximate dN_γ/dE_γ to be a constant, C_i, in such a small energy interval. This approximation enables us to calculate the total log-likelihood of the spectrum $\phi(E)$ from the logarithm of the likelihood map $\mathcal{L}_{ij}$ as

$$\ln \mathcal{L} = \sum_i \ln \mathcal{L}_{ij}|_{\phi_j = \frac{\langle \sigma v \rangle}{8\pi m_\chi^2} \times J \times C_i}. \tag{17}$$

We use the standard Fermi Science Tools package[5] version v10r0p5 to analyze the Fermi-LAT data. We use the newly released Fermi Pass 8 data, with four subsets of different point spread function (PSF) level (i.e., PSF0, PSF1, PSF2 and PSF3), recorded from 4 August 2008 to 4 August 2015. These data are selected from $10^\circ \times 10^\circ$ box regions centered on each dSph, and 500 MeV to 500 GeV for energies to reduce the impact from the bright Earth limb due to the large PSFs at low energies. The events with zenith angles greater than 100° are

[4] The decay case is also included but the default value of J-factor is with open angle 0.1 degree. The result comparing with optimal angle one will be more conservative. Users can generate their own likelihood map with extending source to incorporate J-factor with optimal open angle.

[5] http://fermi.gsfc.nasa.gov/ssc/data/analysis/software/

also excluded. These selected data are divided into 100 × 100 spatial bins with 0.1° bin size and 24 logarithmically spaced energy bins. Using the suggested diffuse background model [6] including a structured Galactic component and an isotropic component, as well as point sources within 15° of each dSph from the third Fermi catalog (3FGL; [48]) as astrophysical background, we first carry out a standard binned likelihood fitting over the entire energy range to get the best-fitting parameters for each point source and the diffuse components. Then we fix all the parameters of diffuse backgrounds and known point sources in the ROI, and add a point source at the position of the dSph. Varying the flux from the newly added point source, we calculate the $\ln \mathcal{L}_{ij}^{kl}$ for the kth dSph and lth subset of data in each energy bin and sum over l to obtain the likelihood map $\mathcal{L}_{ij}^{k}$ for the kth dSph.

B. Combination of many dSphs

If the J-factors of dSphs are known, then we can define a new variable, $\psi_i = \phi_k(E_i)/J_k = \frac{\langle\sigma v\rangle}{8\pi m_\chi^2} \times C_i$, and derive a combined log-likelihood map on the (E, ψ) plane through adding the log-likelihoods of all dSphs together. Fig. 4 shows a combined log-likelihood map on the (E, $E^2\psi$) plane, from the 15 dSphs listed in [41] and their J-factor is taken from Ref. [49]. The solid line shows the one-sided 95% confidence limits obtained from $-2\Delta \ln \mathcal{L}_i = -2(\ln \mathcal{L}_i - \ln \mathcal{L}_i^0) = 2.71$, where $\mathcal{L}_i^0$ is the likelihood for null-hypothesis (i.e., $\psi_i = 0$) for the ith energy bin. For any spectrum $\psi(E)$, the combined log-likelihood can be derived via a sum of log-likelihoods in all energy bins.

However, in general the J-factors of dSphs can not be well determined. In this case we may not be able to have a combined likelihood map as Fig. 4 which is independent of J-factors[7]. We can define a likelihood term due to the uncertainties of J-factors as [41]

$$\mathcal{L}_{J,k}(J_{\rm obs,k}, \sigma_k) = \frac{1}{\ln(10) J_{\rm obs,k}\sqrt{2\pi}\sigma_k} e^{-[\log_{10}(J_k)-\log_{10}(J_{\rm obs,k})]^2/2\sigma_k^2}, \tag{18}$$

where k represents the kth dSph, J_k is the "real" value of the J-factor and $J_{\rm obs,k}$ is the

[6] http://fermi.gsfc.nasa.gov/ssc/data/access/lat/BackgroundModels.html

[7] In Ref. [12] we profile out the likelihoods of J-factors for each energy bin, and obtain a combined likelihood map. This way will multi-count the J-factor uncertainties, though the 95% limit is effected slightly. A proper way should combine first likelihoods in different energy bins and then apply the J-factor likelihoods [39].

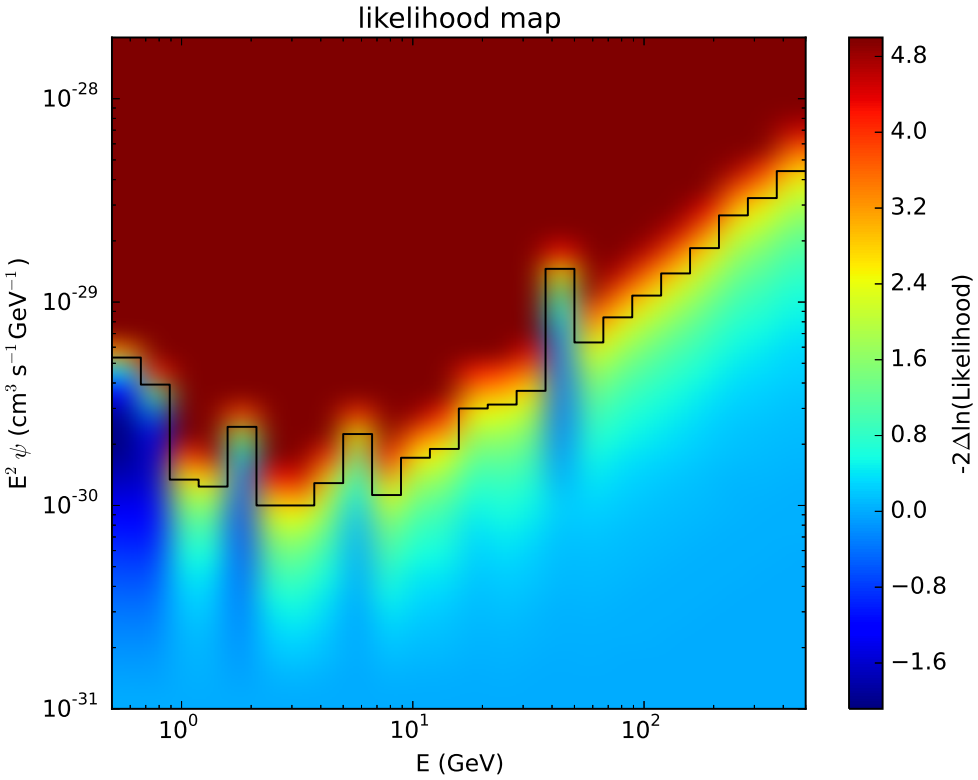

FIG. 4: The log-likelihood map on the (E, $E^2\psi$) plane based on 7-year Fermi-LAT data of the 15 dSphs. The color shows the value of $-2\Delta \ln \mathcal{L}$, normalized individually for each energy bin (see the text for details). The region above the solid line is excluded at the 95% confidence level.

measured J-factor with error σ_k. The joint log-likelihood is then

$$\ln \mathcal{L}(\text{Data}|\phi) = \sum_k \left(\sum_i \ln \mathcal{L}_{ij}|_{\phi_j = \frac{\langle\sigma v\rangle}{8\pi m_\chi^2} \times J \times C_i} + \ln \mathcal{L}_{J,k} \right) . \tag{19}$$

Maximizing the above joint log-likelihood through varying J_k for each dSph, we can obtain the final log-likelihood of the spectrum $\phi(E)$.

In Fig. 5 we show the combinned 95% upper limits for $b\bar{b}$ annihilation channel. Here we use the measurement of J-factors from Ref. [49] to show the importance of including J-factor uncertainty in the upper limits calculation, since σ_k is relatively larger in [49] than that in [39].

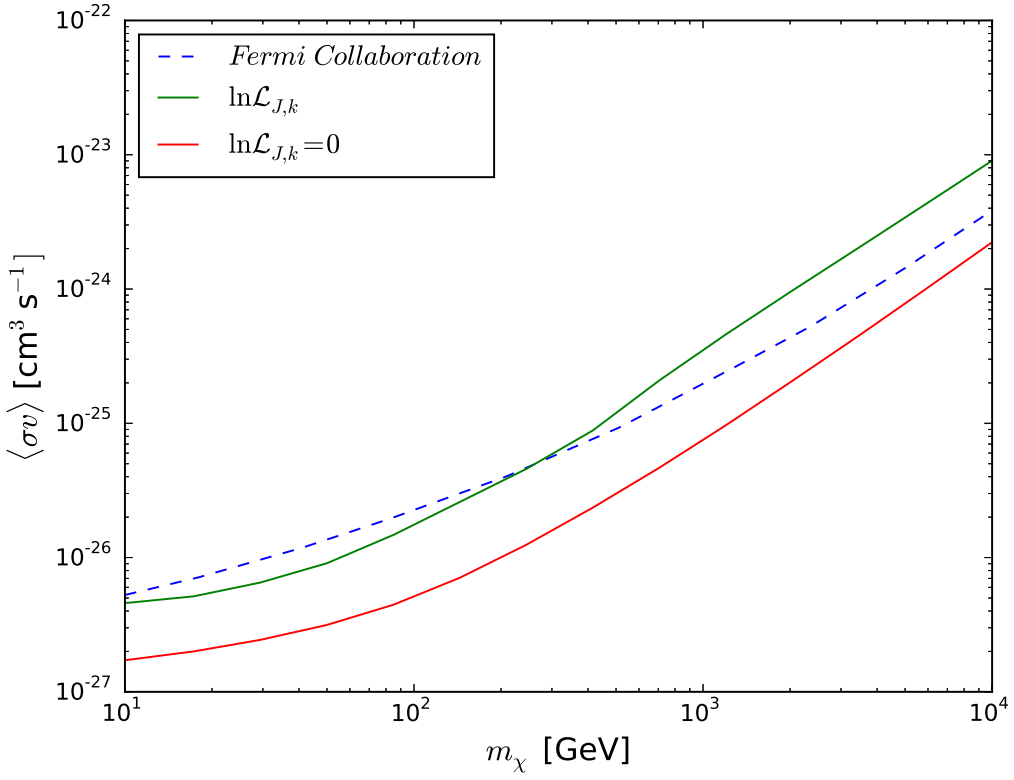

FIG. 5: 95% upper limits of the DM annihilation cross section for the $b\bar{b}$ annihilation channel, derived from a combined analysis of Fermi-LAT observations of 15 dSphs. The result obtained by Fermi-LAT collaboration with 6 year Pass 8 data is shown for comparison [41].

IV. DESCRIPTION TO THE CODE

In this section we describe the structure of the LikeDM code. Users can download the source code from Ref. [50] or the batch file from the ancillary files to this paper in arXiv website. LikeDM is written in `Fortran95`, with `Python` interface available.

A. Installation

LikeDM contains external package `Minuit` [35] to maximize the likelihoods, which needs to be installed first. To install pyLikeDM, "f2py" package is required. We provide a `BASH` script (`create_LikeDM.sh`) to have the quick installation. By running `create_LikeDM.sh`, the user needs to choose the the `pyminuit` installation option in a comment-interface way:

```
./create_LikeDM.sh

+++++++++++++++++++++++++++++++++++++++++++++++++++++++++++++++++++++
Start installing pyminuit
+++++++++++++++++++++++++++++++++++++++++++++++++++++++++++++++++++++
# Two ways to install pyminuit:
# (enter "use_pip" or "local" and other keys for doing nothing.)
local
.
.
.
End installing pyLikeDM
Enjoy use!
```

The only question is to choose the way to install `pyminuit`. There are three options: `use_pip`, `local`, and any other key. If one chooses the flag `use_pip`, the `sudo` authorization is required to install `iminuit` via `pip`. If the user does not have `pip` installed, he/she can install `pyminuit` by using the flag `local`. This step can be skipped if `pyminuit` has already been installed or the user does not want to use the `Python` interface.

LikeDM has been successfully installed and tested under `Scientific Linux`, `Fedora`, and `Ubuntu` operating systems.

B. Running LikeDM

The LikeDM code can be called in the `Python` interface as

```
./pyLikeDM.py LikeDM_input_example.ini [dnde.spec]
```

where `LikeDM_input_example.ini` is an example file of the input parameters (see below part C for details), and the argument `dnde.spec` is optional, depending on the value of the logical parameter `use_pppc4`. If `use_pppc4=T`, then the DM annihilation or decay yield spectrum dN/dE is computed using the `PPPC4` tables [37]. Otherwise, the file `dnde.spec` with the spectrum generated by the user needs to be provided.

C. Inputs and outputs

We provide an example of the input file, `LikeDM_input_example.ini`, in the main folder of LikeDM:

```
.
.
# See all the information?
# 0 for chisq results
# 1 for inputs
# 2 for fitting (alpha,beta)
# 3 for input dNdE
# 4 for propagated fluxes of e+ and pbar
# 5 for individual dSph spectrum
# >=6 for fitting results in each step, very slow!
seebug=0 #debug_level

# Which gamma-ray likelihood MAP you are going to include?
# (The way to generate likelihood map can be found in arxiv 1212.3990)

dsphs_map=./dat/GaLikeMap/likelihood_fix_p8_psf0123.dat
output_name= LikeDM2016

#solor modulation potential
epmod=0.6 #GV, positron
apmod=0.6 #GV, antiproton

# What is the DM halo you want to use during propagation?
WhatHalo=1 #WhatHalo, 1 for NFW, 2 for Einasto and 3 for isothermal

# 6 propagation parameters combination
# See propagation model in 1205.6474.
# 1-6 correspond to Table I from left to right.
WhatGALPROP=2 #propagation parameters combination


use_dSphs=T      # use_dSphs
use_ep=T         # use_ep
use_ap=T         # use_ap


# If users want to compute decaying DM, this flag should be True.
# Then, code will read decay_time instead of sigmav.
decayDM=T

DMmass=104.00
sigmav=1e-25 # sigma v [cm^3/s] for annihilation
decay_time=1e26 # tau [s] for decay

#  T : use PPPC4 Table
#  False : use external Table from 2nd arguement, ./LikeDM.exe LikeDMexample.ini dnde.txt
```

```
use_pppc4= T     # use PPPC4 dnde

# Branch ratio of xx-> SM SM or x -> SM SM
BR_3=0.0 # e
BR_6=0.0 # mu
BR_9=0.0 # tau
BR_12=1.0 # b
BR_16=0.0 # W
BR_19=0.0 # Z
```

This input format is exactly the same as `CosmoMC` [51] and `SuperBayes` [52]. The modules used to read the input file are `src/Read_parameters.py` but we provide module `src/inifile.f90` as an alternative option. The parameters are explained in below:

- `output_name`

  The name of the prefix of output files.

- `seebug`

  An integer number to control the debug information shown on the screen. `seebug=0` for total χ^2; `seebug=6` will print out each χ^2 component for each fitting step; `seebug`≥ 6 will give quite a large amount of outputs, including the charged particle spectra before and after the solar modulation.

- `dsphs_map`

  Likelihood map of dSphs. The full path of the map is needed.

- `epmod` and `apmod`

  Solar modulation potentials in units of GV, for electrons/positrons and protons/antiprotons.

- `WhatHalo`

  An integer number to specify the DM halo profile. 1 for NFW, 2 for Einasto and 3 for isothermal.

- `WhatGALPROP`

  An integer number to determine the propagation parameters. 1 to 6 corresponds to the six sets of propagation parameters given in Ref. [20] (see also Table I of this manual).

- `use_dSphs`, `use_ep`, and `use_ap`

  Logical flags to choose whether or not to use the corresponding data. The current version include Fermi γ-ray data from dSphs, AMS-02 e^+e^- data, and PAMELA $\bar{p}$ data.

- `decayDM`

  Logical flag to determine whether the DM annihilates or decays.

- `DMmass`, `sigmav`, `decay_time`

  The DM mass in GeV, annihilation cross section in $\mathrm{cm}^3\mathrm{s}^{-1}$, and decaying lifetime in s. `sigmav` takes effect when `decayDM=F`, and `decay_time` takes effects when `decayDM=T`.

- `use_pppc4`

  Logical flag to specify whether to use the PPPC4 table to calculate dN/dE. If `F`, an external file needs to be provided by the user. *The file needs to be 4 columns, with E in GeV, $\frac{dN}{dE}\big|_\gamma$ in GeV^{-1}, $\frac{dN}{dE}\big|_{e^+}$ in GeV^{-1}, and $\frac{dN}{dE}\big|_{\bar{p}}$ in GeV^{-1}, respectively.*

- `BR_x`

  Branching ratios for different channels when using PPPC4 table. The identification numbers can be found either in `PPPC4` website or the beginning of `src/PYTHIA_PPPC4.f90`.

The outputs include the computed χ^2 values on the screen, and users can easily modify the code to store their outputs to a file.

D. Package roadmap

The source codes of LikeDM are located in `src/` folder. The main routine is `pyLikeDM.py` for the `Python` interface. We introduce the other routines as several groups by their functionality.

- Initialization and Reading tables

```
src/ReadTable.f90
src/PYTHIA_PPPC4.f90
```

`src/inifile.f90`

The routine `src/ReadTable.f90` reads the tables of the dSph likelihood map, the Green's functions for the propagation of positrons and antiprotons in the Galaxy, and the DM annihilation/decay spectra dN/dE either from PPPC4 (connected with `src/PYTHIA_PPPC4.f90`) or the user supplied external file.

In addition to read the tables, we also collected all the initialization subroutines in `src/ReadTable.f90` module so this module is the heart of LikeDM.

The module `src/inifile.f90` is taken from `CosmoMC` which reads the parameter file, or sets default values of the parameters if user wants to use it.

- Gamma-rays from dSphs

`src/gamma_dSphs.f90`

This module provides the computation of DM annihilation/decay fluxes from a set of dSphs and their combined likelihood. The J-factors of these dSphs have been implemented in the likelihood calculation with a profile likelihood method. As default, a total of 15 dSphs, which are Bootes I, Canes Venatici II, Carina, Coma, Draco, Fornax, Hercules, Leo II, Leo IV, Sculptor, Segue I, Sextans, Ursa Major II, Ursa Minor, and Willman I, are included in the current version of LikeDM. Users can enable or disable some dSphs likelihood by turn on/off the flags `dsphs_use` in `src/ReadTable.f90` module. The J-factors are taken from Ref. [49] for both annihilating DM and decaying DM.

- Charged cosmic rays: background

`src/charge_bkg.f90`

This routine calculates the background fluxes of the e^+e^- and $\bar{p}$ using the empirical formula as described in Sec. II-C.

- Charged cosmic ray: DM e^+ and $\bar{p}$

```
src/charge_lepton.f90
src/charge_antip.f90
```

These two routines compute the propagated fluxes of positrons and antiprotons from DM annihilation or decay, using the Green's function method as described in Sec. II-B.

- Charged cosmic rays: datasets

```
src/charge_data.f90
```

This routine gives the cosmic ray data from AMS-02 [11, 31–33] and PAMELA [34], and returns the calculated χ^2 values for given theoretical fluxes.

- Auxiliary module

```
src/MathLib.f90
src/monitorLikeDM.f90
```

The file `src/MathLib.f90` provides some useful mathematical tools such as the interpolation and integration. We also collected all the output information controlled by flag `seebug` in the file `src/monitorLikeDM.f90`.

V. SUMMARY

We present a publically available tool, LikeDM, for the likelihood calculation of DM models in the experimental data. It enables fast computation of the likelihood of a given DM model (mass, cross section or decay rate, annihilation or decay yield spectrum), without digging into the details of CR propagation, Fermi-LAT data analysis, and related astrophysical backgrounds. This code depends only on the `Minuit` minimization package, and is easy to be installed and run. The code LikeDM also provides a easily framework to link any particle model and Monte-Carlo code to do a global study.

The currently released version (v1.0) contains only the indirect ditection part, including the electron/positron measurements by AMS-02, the antiproton measurements by PAMELA, and the γ-ray observations from dSphs by Fermi-LAT. Further developments with more data, e.g., from the γ-ray observations of the Galactic center and isotropic background, as well as the underground direct detection data, will be carried out soon.

Acknowledgments

the World Premier International Research Center Initiative (WPI), MEXT, Japan (YST).

[1] G. Aad *et al.* [ATLAS Collaboration], Phys. Lett. B **716**, 1 (2012) [arXiv:1207.7214 [hep-ex]].

[2] S. Chatrchyan *et al.* [CMS Collaboration], Phys. Lett. B **716**, 30 (2012) [arXiv:1207.7235 [hep-ex]].

[3] E. Aprile *et al.* [XENON100 Collaboration], Phys. Rev. Lett. **109**, 181301 (2012) [arXiv:1207.5988 [astro-ph.CO]].

[4] D. S. Akerib *et al.* [LUX Collaboration], arXiv:1310.8214 [astro-ph.CO].

[5] Q. Yue *et al.* [CDEX Collaboration], Phys. Rev. D **90**, 091701 (2014) doi:10.1103/PhysRevD.90.091701 [arXiv:1404.4946 [hep-ex]].

[6] M. Xiao *et al.* [PandaX Collaboration], Sci. China Phys. Mech. Astron. **57**, 2024 (2014) doi:10.1007/s11433-014-5598-7 [arXiv:1408.5114 [hep-ex]].

[7] M. Cirelli, Pramana **79**, 1021 (2012) doi:10.1007/s12043-012-0419-x [arXiv:1202.1454 [hep-ph]].

[8] L. Bergstrom, Annalen Phys. **524**, 479 (2012) doi:10.1002/andp.201200116 [arXiv:1205.4882 [astro-ph.HE]].

[9] X. J. Bi, P. F. Yin and Q. Yuan, Front. Phys. China **8**, 794 (2013) doi:10.1007/s11467-013-0330-z [arXiv:1409.4590 [hep-ph]].

[10] O. Adriani *et al.* [PAMELA Collaboration], Nature **458**, 607 (2009) [arXiv:0810.4995 [astro-ph]].

[11] M. Aguilar *et al.* [AMS Collaboration], Phys. Rev. Lett. **110**, 141102 (2013).

[12] Y. -L. S. Tsai, Q. Yuan and X. Huang, JCAP **1303**, 018 (2013) [arXiv:1212.3990 [astro-ph.HE]].

[13] A. Arhrib, Y. L. S. Tsai, Q. Yuan and T. C. Yuan, JCAP **1406**, 030 (2014) doi:10.1088/1475-7516/2014/06/030 [arXiv:1310.0358 [hep-ph]].

[14] A. W. Strong, I. V. Moskalenko and V. S. Ptuskin, Ann. Rev. Nucl. Part. Sci. **57**, 285 (2007) [astro-ph/0701517].

[15] E. S. Seo and V. S. Ptuskin, Astrophys. J. **431**, 705 (1994)

[16] A. W. Strong and I. V. Moskalenko, Astrophys. J. **509**, 212 (1998) [astro-ph/9807150].

[17] D. Maurin, F. Donato, R. Taillet and P. Salati, Astrophys. J. **555**, 585 (2001) [astro-ph/0101231].

[18] A. Putze, L. Derome and D. Maurin, Astron. Astrophys. **516**, A66 (2010) [arXiv:1001.0551 [astro-ph.HE]].

[19] C. Evoli, D. Gaggero, D. Grasso and L. Maccione, JCAP **0810**, 018 (2008) [arXiv:0807.4730 [astro-ph]].

[20] M. Ackermann *et al.* [LAT Collaboration], Astrophys. J. **761**, 91 (2012) [arXiv:1205.6474 [astro-ph.CO]].

[21] M. Ackermann *et al.* [LAT Collaboration], Astrophys. J. **750**, 3 (2012)

[22] J. F. Navarro, C. S. Frenk and S. D. M. White, Astrophys. J. **490**, 493 (1997) [astro-ph/9611107].

[23] J. Einasto, Trudy Astrofizicheskogo Instituta Alma-Ata **5**, 87 (1965)

[24] J. N. Bahcall and R. M. Soneira, Astrophys. J. Suppl. **44**, 73 (1980).

[25] G. Bertone, M. Cirelli, A. Strumia and M. Taoso, JCAP **0903**, 009 (2009) [arXiv:0811.3744 [astro-ph]].

[26] C. S. Shen, Astrophys. J. **162**, L181 (1970).

[27] Q. Yuan, X. J. Bi, G. M. Chen, Y. Q. Guo, S. J. Lin and X. Zhang, Astropart. Phys. **60**, 1 (2015) [arXiv:1304.1482 [astro-ph.HE]].

[28] Q. Yuan and X. J. Bi, Phys. Lett. B **727**, 1 (2013) doi:10.1016/j.physletb.2013.10.010 [arXiv:1304.2687 [astro-ph.HE]].

[29] L. Bergstrom, T. Bringmann, I. Cholis, D. Hooper and C. Weniger, Phys. Rev. Lett. **111**, 171101 (2013) [arXiv:1306.3983 [astro-ph.HE]].

[30] T. Kamae, N. Karlsson, T. Mizuno, T. Abe and T. Koi, Astrophys. J. **647**, 692 (2006)

[Erratum-ibid. **662**, 779 (2007)] [astro-ph/0605581].

[31] L. Accardo *et al.* [AMS Collaboration], Phys. Rev. Lett. **113**, 121101 (2014).

[32] M. Aguilar *et al.* [AMS Collaboration], Phys. Rev. Lett. **113**, 121102 (2014).

[33] M. Aguilar *et al.* [AMS Collaboration], Phys. Rev. Lett. **113**, 221102 (2014).

[34] O. Adriani *et al.* [PAMELA Collaboration], Phys. Rev. Lett. **105**, 121101 (2010) [arXiv:1007.0821 [astro-ph.HE]].

[35] F. James and M. Roos, Comput. Phys. Commun. **10**, 343 (1975). doi:10.1016/0010-4655(75)90039-9

[36] L. J. Gleeson and W. I. Axford, Astrophys. J. **154**, 1011 (1968).

[37] M. Cirelli, G. Corcella, A. Hektor, G. Hutsi, M. Kadastik, P. Panci, M. Raidal and F. Sala *et al.*, JCAP **1103**, 051 (2011) [JCAP **1210**, E01 (2012)] [arXiv:1012.4515 [hep-ph]].

[38] M. Ackermann *et al.* [Fermi-LAT Collaboration], Phys. Rev. Lett. **107**, 241302 (2011) doi:10.1103/PhysRevLett.107.241302 [arXiv:1108.3546 [astro-ph.HE]].

[39] M. Ackermann *et al.* [Fermi-LAT Collaboration], Phys. Rev. D **89**, 042001 (2014) doi:10.1103/PhysRevD.89.042001 [arXiv:1310.0828 [astro-ph.HE]].

[40] A. Geringer-Sameth, S. M. Koushiappas and M. G. Walker, Phys. Rev. D **91**, no. 8, 083535 (2015) doi:10.1103/PhysRevD.91.083535 [arXiv:1410.2242 [astro-ph.CO]].

[41] M. Ackermann *et al.* [Fermi-LAT Collaboration], Phys. Rev. Lett. **115**, no. 23, 231301 (2015) doi:10.1103/PhysRevLett.115.231301 [arXiv:1503.02641 [astro-ph.HE]].

[42] Y. Zhao, X. J. Bi, H. Y. Jia, P. F. Yin and F. R. Zhu, arXiv:1601.02181 [astro-ph.HE].

[43] K. Bechtol *et al.* [DES Collaboration], Astrophys. J. **807**, no. 1, 50 (2015) doi:10.1088/0004-637X/807/1/50 [arXiv:1503.02584 [astro-ph.GA]].

[44] A. Drlica-Wagner *et al.* [DES Collaboration], Astrophys. J. **813**, no. 2, 109 (2015) doi:10.1088/0004-637X/813/2/109 [arXiv:1508.03622 [astro-ph.GA]].

[45] A. Geringer-Sameth, M. G. Walker, S. M. Koushiappas, S. E. Koposov, V. Belokurov, G. Torrealba and N. W. Evans, Phys. Rev. Lett. **115**, no. 8, 081101 (2015) doi:10.1103/PhysRevLett.115.081101 [arXiv:1503.02320 [astro-ph.HE]].

[46] S. Li *et al.*, Phys. Rev. D **93**, no. 4, 043518 (2016) doi:10.1103/PhysRevD.93.043518 [arXiv:1511.09252 [astro-ph.HE]].

[47] M. L. Ahnen *et al.* [MAGIC and Fermi-LAT Collaborations], JCAP **1602**, no. 02, 039 (2016) doi:10.1088/1475-7516/2016/02/039 [arXiv:1601.06590 [astro-ph.HE]].

[48] F. Acero, Astrophys. J. Suppl. **218**, no. 2, 23 (2015). doi:10.1088/0067-0049/218/2/23

[49] V. Bonnivard *et al.*, Mon. Not. Roy. Astron. Soc. **453**, no. 1, 849 (2015) doi:10.1093/mnras/stv1601 [arXiv:1504.02048 [astro-ph.HE]].

[50] http://xxxx

[51] A. Lewis and S. Bridle, Phys. Rev. D **66**, 103511 (2002) doi:10.1103/PhysRevD.66.103511 [astro-ph/0205436].

[52] R. R. de Austri, R. Trotta and L. Roszkowski, JHEP **0605**, 002 (2006) doi:10.1088/1126-6708/2006/05/002 [hep-ph/0602028].